Computational investigations on structural and electronic properties of CuI nanoparticles immobilized on modified poly(styrene-*co*-maleic anhydride), leading to unexpected but an efficient catalyzed synthesis of 1,4-dihydropyridine *via* Hantzsch pyridine synthesis

Majid M. Heravi*, Tayebeh Hosseinnejad*, Niousha Nazari

Department of Chemistry, Alzahra University, Vanak, Tehran, Iran

Corresponding authors:

Majid M. Heravi, Fax: +982188041344; Tel: +989121329147; E-mail: mmh1331@yahoo.com.

Tayebeh Hosseinnejad, Fax: +982188041344; Tel: +989124775800; E-mail: tayebeh.hosseinnejad@gmail.com

Abstract:

A quantitative description for the interaction of Cu(I) with poly(styrene-*co*-maleic anhydride) modified with 4-aminopyridine (denoted as CuI/SMI complex) is presented using density functional theory(DFT)and quantum theory of atoms in molecules (QTAIM)approaches. Topological analysis of electron density revealed the existence of effective interactions between Cu(I) ions and the nitrogen in the pyridine ring. Interestingly, the results also showed there is a considerable interaction between Cu(I) and oxygen of carbonyl motif in SMI ligand. Thus, CuI/SMI was examined as a heterogeneous and recyclable catalyst in Hantzsch pyridine synthesis under solvent-free conditions affording diverse 1,4-dihydropyridines (1,4-DHPs) in excellent yields and in the relatively short reaction times.

Keywords: CuI/SMI nanocatalyst, Density functional theory, Quantum theory of atoms in molecules, Hantzsch pyridine synthesis, Green chemistry.

1. Introduction

Copper-catalyzed reactions have gained increasing attentions in modern organic chemistry.[1-4] In general, there are two important kinds of functions for these catalysts in organic reactions. First, the reaction proceeds smoothly and rapidly in the presence of catalyst, for instance, CuI-catalyzed intramolecular *o*-vinylation of carbonyl compounds.[5]Second, when a copper catalyst catalyzes the reaction conventionally, in the same time, it controls the selectivity of the reaction.[6-8] In some special Cu-catalyzed reactions, the regioselectivity is also controlled. One of the most important Cu-catalyzed reactions is the azide-alkyne 1,3-dipolar cycloaddition reaction (entitled as CuAAC reactions) leading to the highly regioselective synthesis of 1,4-disubstituted 1,2,3-triazoles, coined as "Click Reaction" by Sharpless *et al.*[4] This reaction has been extensively studied during the past decade from different points of view[9,10] including the computational assessments of origins and prediction of its regioselectivity which we have recently highlighted them in a comprehensive review.[11] In addition, a massive number of experimental and computational developments in this area has confirmed the coordination of Cu(I) to C-C triple[12] and double bonds during the reaction.[13]Cu(I) can also coordinate to several nitrogen heterocycles including pyridine which can efficiently catalyze several diverse organic transformations.[14-24]

In continuation of our interest on development of heterogeneous nanocatalysts and their applications,[25-36] we recently reported the synthesis, characterization and catalytic activity of CuI nanoparticles immobilized on poly(styrene-*co*-maleic anhydride) modified by 2-amino and 4-aminopyridine,[37,38] and used them successfully in the regioselective synthesis of 1,2,3-triazoles through Huisgen 1,3-dipolar cycloaddition[39] *via* click reaction.[40]For being more insightful, we also computationally assessed metal-ligand interactions for interpretation of some of our experimental observations.[41-47]

In this light and due to our interest, we decided to study a quantitative description for structural and electronic features of metal-ligand interactions in poly(styrene-*co*-maleic anhydride) copper complex model (CuI/SMI)modified with 4-aminopyridine using density functional theory (DFT)[48] and quantum theory of atoms in molecules (QTAIM)approaches. [49] Encouraged byour interestingobtained computational data, weprepared our Cu(I) nanoparticles immobilized on poly(styrene-co-maleic anhydride) modified with 4-aminopyridine[38] and identified it *via* FT-IR and inductively coupled plasma (ICP) methods which was in agreement with that of previously well-documented compound.[38] Then, we examined the catalytic activity of CuI/SMI in the Hantzsch pyridine synthesis. Herein, we wish to reveal our computational results which led to the highly efficient, green and high yielding Cu(I)-catalyzed synthesis of a wide range of DHPs *via* Hantzsch reaction (Scheme 1).

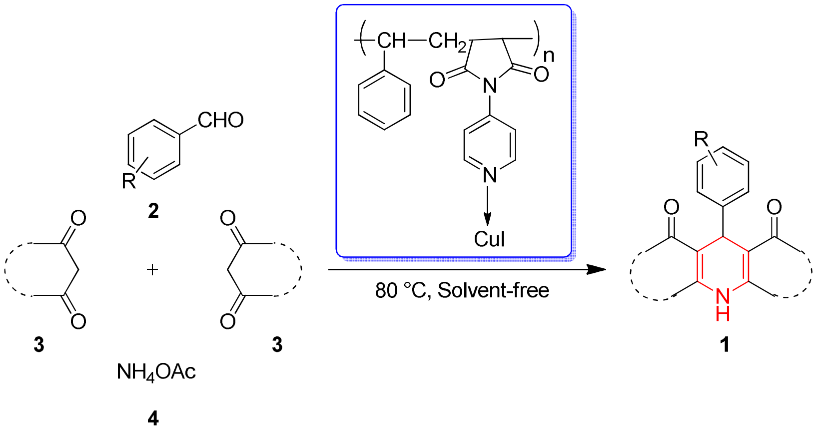

Scheme 1. General synthesis of 1,4-dihyropyridine derivatives **1**

2. Experimental

2.1. Materials and Methods

All chemicals and solvents were purchased from Merck and Aldrich chemical companies and used without further purification. Melting points were determined on an Electrothermal 9200-Barnstead apparatus and were uncorrected. IR spectra were obtained using a FT-IR Tensor 27 spectrometer instrument and samples were prepared as KBr plates. ^{1}H NMR and ^{13}C NMR spectra were recorded on a Bruker Ultrashield 400 Avance III spectrometer at 400 MHz using DMSO-d$_6$ as a solvent with tetramethylsilane (TMS) as an internal standard. Mass spectra were measured with Network mass selective detector (Agilent) 6890/5973. Most compounds were known and their physical data were compared with those reported previously and found being identical.

2.2. Preparation of CuI/SMI Catalyst

The catalyst was prepared in accordance with our previous procedure[38] as follows**.** In a 100 ML glass reactor SMA (1.00 g), 4-aminopyridine (1.54 g, 16 mmol) and dry DMF (15 ml) were placed and then oxygen purged by charging N$_2$ gas into the reactor and sealed. This reactor was placed into a thermostatic oil bath and the reaction mixture was oscillated until the reagents were dissolved in DMF. Then the reaction mixture was oscillated at 35 ºC for 3.5 h. Then, acetic anhydride (0.6 ml, 6 mmol), sodium acetate (0.33 g, 4 mmol), and triethylamine (0.3 ml, 2 mmol) were added into the reactor using syringe. Then the temperature was raised to 75ºC and oscillating was continued for 3.5 h. The reaction mixture was then cooled to ambient temperature and poured into 300 ml of vigorously stirring methanol, slowly. The formed fiber-like precipitated polymer was washed with methanol and dried under reduced pressure at 70ºC to constant weight.

CuI (0.247 mg, 0.001 mmol) was dissolved in CH_3CN (2 ml) under ultrasonic irradiation and stirring, to give a transparent pale yellow solution. DMF (20 ml) was then added at ambient temperature to give CuI NPs. To this mixture, dry SMI (1.000 g) was added. Then the mixture was magnetically stirred at reflux temperature for 5 h under the atmosphere of nitrogen. The solid was washed with CH_3CN and dried under vacuum at 60ºC to obtain the CuI/SMI. The synthesized CuI/SMI was identified by comparison of its FT-IR spectrum with the authentic compound and found identical. Moreover, the copper content of the polymer-supported catalyst was determined by ICP analysis and found being 6.92% w/w and used to measure the amount of copper content after five consecutive runs, too.

2.3. Synthesis of 1,4-DHPs: General Procedure

In a round-bottomed flask, an appropriate aromatic aldehyde **2** (1 mmol), a suitable*β*-dicarbonyl compound**3** (2 mmol), ammonium acetate **4** (1.5 mmol) and CuI/SMI nanocatalyst (0.04 g) were thoroughly mixed. Then, the mixture was heated in an oil-bath at 80 °C with concomitant stirring. The progress of reaction was monitored by TLC (EtOAc:*n*-hexane; 4:1). After completion of the reaction, the mixture was cooled to room temperature, then hot ethanol was added and the catalyst was easily filtered off under reduced pressure. The filtrate was evaporated to dryness and the crude was recrystallized from ethanol in 81-93% yields, calculated based on the starting aldehyde. The spectroscopic and analytical data for new products and some selected known compounds are presented as follows. The rest are provided as supplementary.

Ethyl 4-(4-chlorophenyl)-2,7,7-trimethyl-5-oxo-1,4,5,6,7,8-hexahydroquinoline-3-carboxylate (1b):

M.p.244-246 °C.IR (KBr): 3275, 3070, 2964, 1706, 1646 cm^{-1}.^1H NMR (300 MHz, $CDCl_3$): 0.67 (s, 3H), 0.83 (s, 3H), 0.95 (t, 3H), 1.85 (d, 1H), 1.96 (d, 1H), 2.05 (d, 1H), 2.10-2.13 (m, 4H), 3.79(q, 2H), 4.73 (s, 1H), 6.89-7.01 (m, 4H), 8.17 (s, 1H) ppm.MS (m/e): 373 (M+).

Ethyl 4-(4-methoxyphenyl)-2,7,7-trimethyl-5-oxo-1,4,5,6,7,8-hexahydroquinoline-3-carboxylate (1c):

M.p.255-256 °C.IR (KBr):3276, 2956, 1703, 1648, 1606, 1469, 1381, 1215, 1031, 765 cm^{-1}.^1H NMR (300 MHz, $CDCl_3$): 0.71 (s, 3H), 0.85 (s, 3H), 0.98 (t, 3H), 1.87 (d, 1H), 1.97 (d, 1H), 2.06 (d, 1H), 2.11-2.15 (m, 4H), 3.51 (s, 3H), 3.81 (q, 2H), 4.71 (s, 1H), 6.57-6.98 (m, 4H), 8.02 (s, 1H) ppm.MS (m/e): 369 (M+).

9-(3-Fluorophenyl)-3,3,6,6-tetramethyl-3,4,6,7,9,10-hexahydroacridine-1,8(2*H*,5*H*)-dione (1h):

M.p.298-300°C.IR (KBr): 3279, 3069, 2956, 1636, 1218 cm^{-1}.^{1}H NMR (400 MHz, DMSO-d_6): 0.87 (s, 6H), 1.01 (s, 6H), 2.01 (d, *J* = 16.4 Hz, 2H), 2.18 (d, *J* = 16 Hz, 2H), 2.35 (d, *J* = 17.6 Hz, 2H), 2.45 (d, *J* = 16.8 Hz, 2H), 4.82 (s, 1H), 6.84-7.23 (m, 4H), 9.37 (s, 1H) ppm.MS (m/e): 367 (M+).

9-(4-Chlorophenyl)-3,3,6,6-tetramethyl-3,4,6,7,9,10-hexahydroacridine-1,8(2*H*,5*H*)-dione (1i):

M.p.293-295°C.^{1}H NMR (400 MHz, DMSO-d_6): 0.97 (s, 6H), 1.09 (s, 6H), 2.17 (d, *J* = 16.4 Hz, 2H), 2.23 (d, *J* = 11.6 Hz, 2H), 2.27 (d, *J* = 11.2 Hz, 2H), 2.34 (d, *J* = 16.8 Hz, 2H), 5.06 (s, 1H), 7.16-7.18 (m, 2H), 7.28-7.30 (m, 2H), 7.33 (s, 1H) ppm.^{13}C NMR (DMSO-d$_6$, 400 MHz): 27.1, 29.5, 32.7, 33.3, 40.9, 50.7, 113.1, 128.1, 129.5, 131.5, 145.1, 148.5, 195.7 ppm.

Diethyl 4-(4-chlorophenyl)-2,6-dimethyl-1,4-dihydropyridine-3,5-dicarboxylate (1p):

M.p.145-147°C.^{1}H NMR (400 MHz, DMSO-d_6): 1.24 (t, 6H), 2.34 (s, 6H), 4.06-4.11 (m, 2H), 4.12-4.15 (d, 2H), 4.97 (s, 1H), 5.73 (s, 1H), 7.17-7.21 (m, 2H), 7.22-7.28 (m, 2H) ppm.^{13}C NMR (DMSO-d$_6$, 400 MHz): 14.3, 19.6, 39.2, 59.8, 103.9, 127.9,129.4, 131.7, 143.9, 146.3, 167.4 ppm.

3. Results and Discussion

3.1. Computational section

We initially concentrated on the nature of interactions between copper metal ions and SMI ligand modified with 4-aminopyridinein the aforementioned polymer-supported copper complex *via* DFT computations. First, we presented a comparative assessment on metal-ligand interactions in the gas and solution phases to investigate the solvent effect on experimental affordance of CuI/SMI complexation reaction.[38] In this respect, an effective computational model for SMI ligand and CuI/SMI complex was designed (Scheme2).As illustrated in Scheme2, two coordinating modes were modeled for the description of metal-ligand interactions denoted as N-CuI/SMI (copper coordinates to pyridine nitrogen) and O-CuI/SMI(copper coordinates to carbonyl oxygen), respectively. On the other hand, our proposed computational model has a reputable embody between accuracy and time saving efficiency of computational procedure.

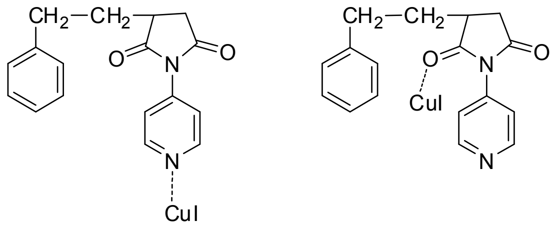

N-CuI/SMI complex O-CuI/SMI complex

Scheme 2. A simple model for two coordinating modes in polymer-supported copper catalyst

DFT computations were performed at M06/6-31G*theory level to determine the optimized structure of SMI ligand and N-CuI/SMI and O-CuI/SMI complexes. The harmonic frequency analysis was employed to confirm the found structures correspond to minima. It is noteworthy to mention that M06 functional[50]has been introduced recently as a hybrid meta-GGA (generalized gradient approximation) exchange-correlation functional, parameterized including both transition metals and nonmetals and was recommended for application in organometallic and inorganometallic thermochemistry, kinetic studies and non-covalent interactions. All DFT computations were performed using GAMESS suite of programs.[51]Theenergy minimized structure of SMI ligand and N-CuI/SMI and O-CuI/SMI complexes calculated at M06/6-31G* theory level have been displayed in Figure1.

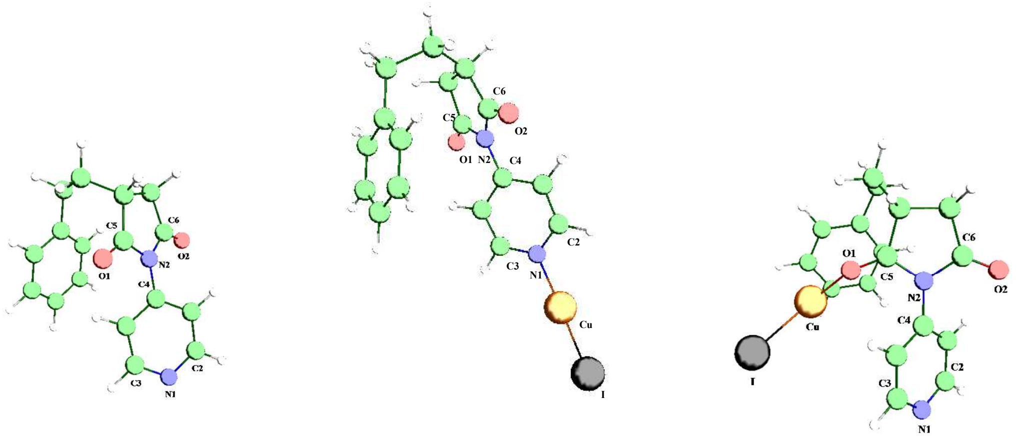

SMI ligand **N-CuI/SMI complex** **O-CuI/SMI complex**

Figure1.

In order to characterize the variation of bond orders *via* complexation process and interpret the interaction strength between copper ion and SMI ligand, we have also compared the bond order of some selected key bonds in SMI ligand with its corresponded bonds in N-CuI/SMI and O-CuI/SMI complexes. In Table 1, we have listed bond order and bond length of some selected chemical bonds in the coordination sphere calculated at M06/6-311+G** theory level. The reported results in Table 1 indicate two facts as follows: i) decreasing in the bond order of carbonyl group and also C−N of pyridine ring through complexation (C5-O1 bond order from 2.440 in SMI ligand to 2.352 in O-CuI/SMI complex and also N1-C2 and N1-C3 bond order from 1.339 and 1.391 in SMI ligand to 1.317 and 1.288 in N-CuI/SMI complex, respectively)that can mainly be ascribed to the donation of shared electrons from these chemical bonds to copper ions and is in agreement with the reported FT-IR spectroscopic observations,[38] ii) Cu-N interaction is stronger than Cu-O interaction (0.512 and 0.171 for calculated Cu-N and Cu-O bond order, respectively). On the basis of the obtained results, we can predict that copper nanoparticles will bind more effectively to pyridinic nitrogen than carbonyl oxygen.It is important to note that the variation in the calculated bond order values correlates with trend of bond distance change through the complexation process.

<Table 1>

In the next step, we have focused on another significant feature in the affordance of synthesis of CuI/SMI complex; solvent effect. In this content, we comparatively evaluated the bond orders of Cu-N and Cu-O in the presence of ethanol and dimethylformamide (DMF) as solvents. It is important to mention that in an independent work, we have experimentally observed a more effective immobilization and smaller size of CuI nanoparticles on SMI support modified with 4-aminopyridinein DMF solution in comparison with ethanol.[38]

The solvent effect computations were performed *via* polarized continuum model (PCM)[52]at M06/6-311+G** theory level. In Table 2, we have presented comparatively the calculated bond orders of Cu-N and Cu-O chemical bonds in DMF and ethanol solution phases. The reported result of Table 2 confirms more strength of Cu-N bond than Cu-O in solution phase. Moreover, the bond orders in N-CuI/SMI and O-CuI/SMI complexes have larger calculated values in DMF solution in comparison with those in ethanol which corroborate the observed practical preference of DMF as solvent rather than ethanol.[38]

<Table 2>

In order to explicate the nature of metal-ligand interactions in CuI/SMI, we concentrated on topological study of electron density *via* QTAIM method.[48,49]In this respect, resulting M06/6-311+G** wave function files for the optimized structures of SMI ligand, N-CuI/SMI and O-CuI/SMI complexes were used as inputs to AIM2000 program package.[53] Then, we focused on the calculation of some selected bond critical points (BCPs) and their associated bond paths to perform a comparative survey on the bond strength from the electronic point of view.

The calculated values of electron density (ρ_b), its laplacian ($\nabla^2\rho_b$), electronic kinetic energy density (G_b), electronic potential energy density (V_b), total electronic energy density (H_b), and $|V_b|/G_b$ of some selected critical points for SMI ligand, N-CuI/SMI and O-CuI/SMI complexes were listed in Table3. QTAIM molecular graphs of SMI ligand, N-CuI/SMI and O-CuI/SMI complexes including all bond and ring critical points and their associated bond paths were also displayed in Figure2.

<Table 3>

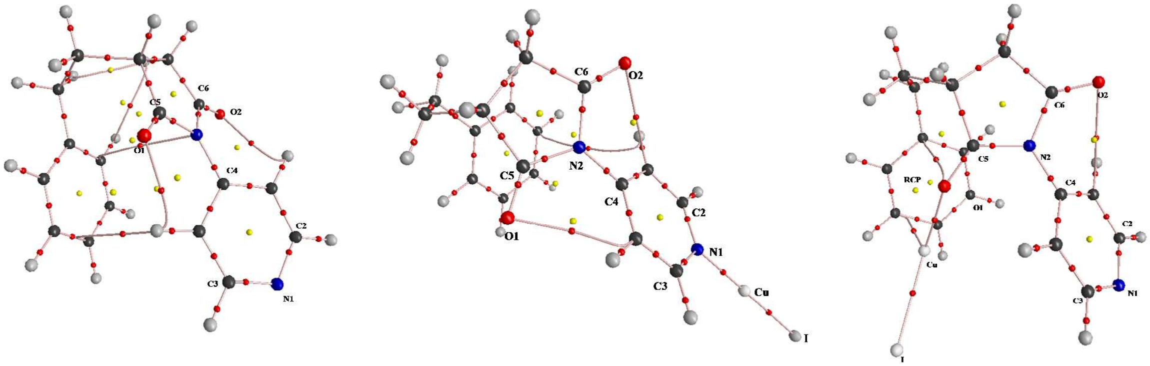

SMI ligand **N-CuI/SMI complex** **O-CuI/SMI complex**

Figure2.

The following two facts can be deduced from the comparative assessment of the reported results of Table 3: i) the large positive values of electron density together with the negative values of $\nabla^2\rho_b$ and H_b and also $|V_b|/G_b >$ 2 values on C=O and C−N BCPs approbate the covalent character of these chemical bonds in SMI ligand, N-CuI/SMI and O-CuI/SMI complexes. However, at Cu-N, Cu-O and Cu-I BCPs, the small values of electron density with the positive values of $\nabla^2\rho_b$ and small negative values of H_b and also $1 < |V_b|/G_b < 2$ calculated values indicate the presence of semi covalent-electrostatic interactions ii) decreasing in the calculated values of ρ_b at C=O and C−N BCPs *via* complexation affirms the donation of shared electrons to the metal center and is in confirmation with reducing in the stretching frequency of IR spectrum iii) comparison of the calculated electron density values of Cu-N and Cu-O BCPs in N-CuI/SMI and O-CuI/SMI complexes uphold that interaction of copper cation with pyridinic nitrogen is stronger than oxygen of carbonyl group. As illustrated in Figure 2, a more stringent assessment on QTAIM wave function analysis demonstrates that the weaker Cu-O interaction in O-CuI/SMI complex can mainly be attributed to the presence of BCPs between carbonyl oxygen and also copper ion with facing phenyl carbon atoms. These interactions lead to the formation of new ring critical point (denoted as RCP in QTAIM molecular graph of O-CuI/SMI complex in Figure 2) and consequently the electron density of Cu-O BCP is distributed in the aforementioned ring and therefore decreased.

Although all our obtained computed results in the both gas and solution phases demonstrate that the interaction between CuI nanoparticles with pyridinie nitrogen of SMI ligand is stronger than that of oxygen of carbonyl group, delightfully we found that the possibility for the formation of O-CuI/SMI is also enough to be considered and not being over looked. This phenomenon has been realized previously.[54] Moreover, it should be mentioned that our DFT and QTAIM computational assessments on the interactions between CuI nanoparticles and poly(styrene-*co*-maleic anhydride) modified by 2-aminopyridine have demonstrated the similar behavior from the electronic viewpoint.[37] Based on our obtained computational results, we were prompted to examine the catalytic activity of CuI/SMI polymeric support in a name reaction so called “Hantzsch Pyridine Synthesis” as a well-known approach with the well-established mechanism for the synthesis of DHPs as an important biologically active compounds.[55,56]

In virtually all suggested mechanism for Hantzsch pyridine synthesis, carbonyl group of aldehyde as a starting material is initially activated which makes it susceptible for being attacked by nucleophiles leading to the production of corresponding1,4-DHPs.

3.2. Synthesis of 1,4-DHP derivatives

Initially, a one-pot four-component reaction of benzaldehyde, ethyl acetoacetate, dimedone and ammonium acetate was selected as a model reaction. This reaction was performed in the presence of CuI/SMI in water as a solvent to obtain the corresponding dihydropyridine**1a**. In order to optimize the experimental conditions for the model reaction, we studied the effects of solvents and temperatures in the presence of CuI/SMI. As shown in Table 4, among the tested solvents such as water, ethanol, acetonitrile, mixture of H_2O/EtOH (1:1) and solvent-free conditions, the solventless system gave the best output in terms of time, temperature and yield (30 min at 80 °C under solvent-free conditions, yield 92%) (Entry2). Conducting the reaction under lower temperature (60 °C) led to obvious decrease in the yield of the desired product (Entry1).

<Table 4>

In the next step, the model reaction was carried out using different quantities of CuI/SMI. Table 5 illustrates that the best yield has been achieved when 0.04 g of CuI/SMI was used as the optimum amount (Entry 3). By decreasing the amount of CuI/SMI as catalyst, the reaction time should be increased for obtaining the similar yield (Entries 1 and 2). Using the higher amounts of catalyst has generally no effect on outcome of the model system (Entry 4).

<Table 5>

When the optimal reaction conditions were secured, we examined the generality and substrate scope of this reaction. Divers *β*-dicarbonyl compounds**3** were reacted with a wide variety of aldehydes **2** and ammonium acetate **4** in the presence of CuI/SMI as catalyst in solvent-free conditions to obtain the corresponding desired products**1** in good to excellent yields. The results are summarized in Table 6. Under the optimal reaction conditions, the reactions were completed within 25-45 minutes. By using this effective nanocatalyst, the aldehydes carrying both electron-donating groups such as methyl and methoxy and electron-withdrawing groups such as nitro and halide gave products in good to excellent yields.

<Table 6>

To study the recyclability and reusability of the catalyst, we repeated the model reaction under optimized reaction conditions. After the completion of the model reaction, the mixture was filtered and thoroughly washed with acetone. The catalyst was dried under reduced pressure at 70 °C for 3 h and being reused for subsequent run. We found that the catalyst can effectively be reused for at least 5 cycles without any significant loss in its catalytic activity or the yield of products (Figure3).

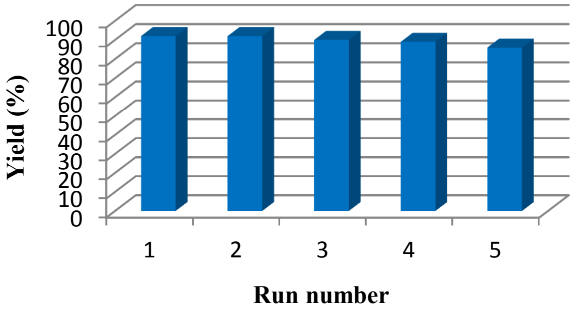

Figure3.

The possible mechanism for the synthesis of substituted 1,4-DHP derivatives **1** catalyzed by copper catalyst is proposed as illustrated in Scheme3. The synthesis of 1,4-DHPs **1**beginswith the Knoevenagel condensation of the activated aldehyde **2**and *β*-dicarbonyl compound**3**using Cu(I), and proceeds through a Michael addition of the second equivalent of activated methylene compound **3** into the Knoevenagel intermediate **5**. After the formation of enamine intermediate **6**, intramolecular cyclization gives the desired product **1**. The important role of copper catalyst is vividly observed in the first and second step where it catalyzes the Knoevenagel condensation and Michael addition, respectively.

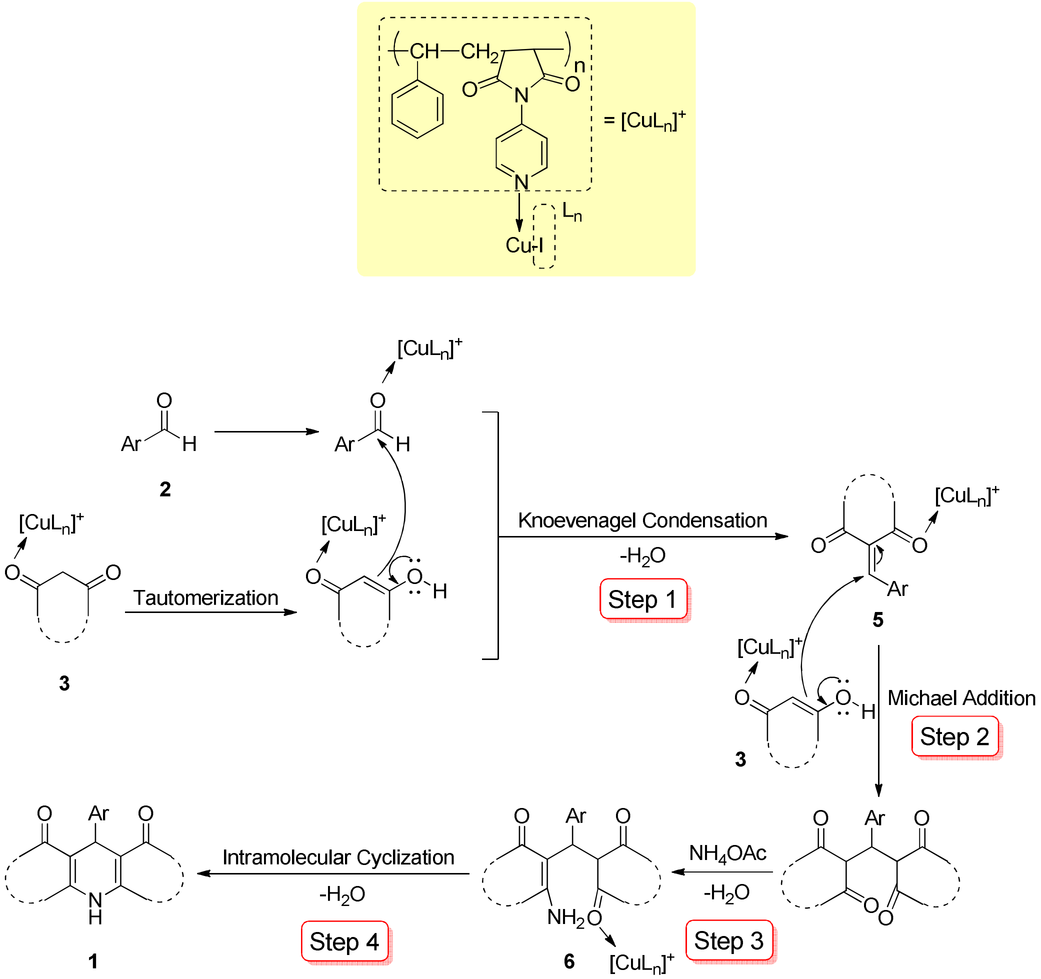

Scheme 3. Plausible mechanism for the synthesis of substituted 1,4-DHP derivatives

4. Conclusion

In summary, we have made a comparative assessment on structural and electronic features of metal-ligand interactions in poly(styrene-*co*-maleic anhydride) copper complex models (CuI/SMI) modified with 4-aminopyridine using DFT and QTAIM approaches. Strictly speaking, we focused on theoretical interpretation of metal-ligand interaction strength in the gas and solution phases to analyze experimental observations in terms and conditions of immobilization of copper nanoparticles on SMI. In overall, our obtained computed results demonstrated that the interaction between CuI nanoparticles and pyridine nitrogen of SMI ligand is stronger than oxygen of carbonyl group, but the possibility for the formation of O-CuI/SMI complex is also considerable and should not be over looked. The interaction between CuI nanoparticles and carbonyl group was good enough to accelerate a classical name reaction so called Hantzsch pyridine synthesis. In this computational context, we examined the catalytic activity of CuI/SMI in Hantzsch reaction to interact and activate aldehyde species for producing 1,4-DHPcompounds.

Thus, we have developed an efficient, facile and green method utilizing CuI/SMI as catalyst for a one-pot synthesis of various types of 1,4-DHPs *via* a multi-component reaction under solvent-free conditions which is also important from the green chemistry viewpoint. Furthermore, wide scope, simple operation, high yields, short reaction times, simple work-up and reusing the catalyst at least for five consecutive runs without any pre-activation and any appreciable loss of activity are other advantages and merits of the present method. In conclusion, CuI/SMI can be introduced as an effective and recyclable catalyst in Hantzsch pyridine synthesis for the synthesis of a wide range of substituted 1,4-DHP derivatives. Examination of activity for this catalyst in other catalytic reactions involving at least one compound bearing a carbonyl group is underway in our laboratory.

Acknowledgment

We are thankful to Alzahra university research council for partial financial supports. Tayebeh Hosseinnejad is also thankful to Iran National Science Foundation (INSF) for its financial support.

References

1. Speers, A. E.;Adam, G. C.;Cravatt, B. F. *J. Am. Chem. Soc.***2003**, *125*(16), 4686.doi: 10.1021/ja034490h.

2. Beatty, K. E.;Xie, F.;Wang, Q.;Tirrell, D. A. *J. Am. Chem. Soc.***2005**, *127*(41), 14150.doi: 10.1021/ja054643w.

3. Deiters, A.;Schultz, P. G. *Bioorg. Med. Chem. Lett.***2005**, *15*(5), 1521.doi: 10.1016/j.bmcl.2004.12.065.

4. Golas, P. L.;Tsarevsky, N. V.;Sumerlin, B. S.;Matyjaszewski, K. *Macromolecules***2006**, *39*(19), 6451.doi: 10.1021/ma061592u.

5. Fang, Y.;Li, C.*Chem. Commun.***2005**, (28), 3574.doi: 10.1039/B505006E.

6. Sromek, A. W.;Rubina, M.;Gevorgyan, V. *J. Am. Chem. Soc.***2005**, *127*(30), 10500.doi: 10.1021/ja053290y.

7. Zhang, L.;Ye, D. J.;Zhou, Y.;Liu, G. N.;Feng, E. G.;Jiang, H. L.;Liu, H. *J. Org. Chem.***2010**, *75*(11), 3671.doi: 10.1021/jo100378u.

8. Xia, Y. Z.;Dudnik, A. S.;Gevorgyan, V.;Li, Y. H. *J. Am. Chem. Soc.***2008**, *130*(22), 6940.doi: 10.1021/ja802144t.

9. Heina, J. E.;Fokin, V. V. *Chem. Soc. Rev.***2010**, *39*(4), 1302.doi: 10.1039/B904091A.

10. Heravi, M.M.; Tamimi, M.; Yahyavi, H.; Hosseinnejad, T. *Curr. Org. Chem.* **2016**, *20*(1),1591.doi: 10.2174/1385272820666151217183010.

11. Hosseinnejad, T.;Fattahi, B.; Heravi, M. M. *J. Mol. Model.***2015**, *21*(10), 1. doi: 10.1007/s00894-015-2810-2.

12. Meldal, M.;Tornøe, C. W. *Chem. Rev.***2008**, *108*(8), 2952.doi: 10.1021/cr0783479.

13. Bellott, B. J.;Girolami, G. S. *Organometallics***2009**, *28*(7), 2046.doi: 10.1021/om801078c.

14. Jia, J.;Jiang, C.;Zhang, X.;Jiang, Y.;Ma, D. *Tetrahedron Lett.***2011**, *52*(43), 5593.doi: 10.1016/j.tetlet.2011.08.059.

15. Ghasemzadeh, M. A.;Safaei-Ghomi, J. *ActaChim. Slov.***2015**, *62*(1), 103.doi: 10.17344/acsi.2014.775.

16. Chavan, P. V.;Pandit, K. S.;Desai, U. V.;Kulkarni, M. A.;Wadgaonkar, P. P. *RSC Adv.***2014**,*4*(79), 42137.doi: 10.1039/C4RA05080K.

17. Safaei-Ghomi, J.;Ghasemzadeh, M. A. *J. Sulfur Chem.***2013**, *34*(3), 233.doi: 10.1080/17415993.2012.728220.

18. Kumari, K.;Singh, D.;Singh, K. N. *Tetrahedron***2013**, *69*(1), 82.doi: 10.1016/j.tet.2012.10.066.

19. Mishra, S.;Ghosh, R. *Synthesis***2011**, *2011*(21), 3463.doi: 10.1055/s-0030-1260255.

20. Balogh-Hergovich, É.;Speier, G. *React. Kinet. Catal. Lett.***1975**, *3*(2), 139.doi: 10.1007/BF02187505.

21. Li, Z.;Hong, J.;Zhou, X. *Tetrahedron***2011**, *67*(20), 3690.doi: 10.1016/j.tet.2011.03.067.

22. Liu, Z.;Qayyum, M. F.;Wu, C.;Whited, M. T.; Djurovich, P. I.;Hodgson, K. O.;Hedman, B.;Solomon, E. I.;Thompson, M. E. *J. Am. Chem. Soc.***2011**, *133*(11), 3700.doi: 10.1021/ja1065653.

23. Braga, D.;Grepioni, F.;Maini, L.;Mazzeoa, P. P.;Ventura, B. *New J. Chem.***2011**, *35*(2), 339.doi: 10.1039/C0NJ00547A.

24. Wang, D.;Ding, K. *ChemCommun (Camb).***2009**, (14), 1891.doi: 10.1039/B821212K.

25. Heravi, M. M.;Ghobadi, N. *ScientiaIranica***2015**, *22*(3), 911.

26. Nemati, F.;Heravi, M. M.;Elhampour, A. *RSC Adv.***2015**, *5*(57), 45775.doi: 10.1039/C5RA06810J.

27. Bamoharram, F. F.;Hashemi, S.;Heravi, M. M.;Rashidi, H.; Ayati, A. *Curr.Nanosci.***2014**, *10*(5), 736.doi: 10.2174/1573413710666140129234519.

28. Bamoharrama, F. F.;Heravi, M. M.;Saneinezhad, S.;Ayati, A. *Prog. Org. Coat.***2013**, *76*(2-3), 384.doi: 10.1016/j.porgcoat.2012.10.005.

29. Nemati, F.;Heravi, M. M.;Saeedi Rad, R. *Chinese J. Catal.***2012**, *33*(11-12), 1825.doi: 10.1016/S1872-2067(11)60455-5.

30. Heravi, M. M.;Alishiri, T. *Heterocycles***2012**, *85*(3), 545.doi: 10.3987/REV-11-725.

31. Bamoharram, F. F.;Heravi, M. M.;Ebrahimi, J.;Ahmadpour, A.;Zebarjad, M. *Chinese J. Catal.***2011**, *32*(5), 782.doi: 10.1016/S1872-2067(10)60219-7.

32. Heravi, M. M.;Tavakoli-Hoseini, N.;Bamoharram, F. F. *Bulg. Chem. Commun.***2011**, *43*(3), 423.

33. Heravi, M. M.;Tavakoli-Hoseini, N.;Bamoharram, F. F. *Green. Chem. Lett. Rev.***2010**, *3*(4), 263.doi: 10.1080/17518251003749387.

34. Heravi, M. M.;Sadjadi, S.;Sadjadi, S.;Oskooie, H. A.;Bamoharram, F. F. *Ultrason. Sonochem.***2009**, *16*(6), 708.doi: 10.1016/j.ultsonch.2009.02.010.

35. Heravi, M. M.;Sadjadi, S.;Sadjadi, S.;Oskooie, H. A.;Bamoharram, F. F. *Ultrason. Sonochem.***2009**, *16*(6), 718.doi: 10.1016/j.ultsonch.2009.04.004.

36. Bamoharram, F. F.;Heravi, M. M.;Roushani, M.;Toosi, M. R.;Jodeyre, L. *Green. Chem. Lett. Rev.***2009**, *2*(1), 35.doi: 10.1080/17518250902998095.

37. Baeilashaki, T.; Oskooie, A. H.; Hosseinnejad, T.; Heravi, M. M. *J. Coord. Chem.***2016**, Submitted.

38. Hashemi, E.;Beheshtiha, S. Y.;Ahmadi, S.;Heravi, M. M. *Transition Met. Chem.***2014**, *39*(5), 593.doi: 10.1007/s11243-014-9838-5.

39. Huisgen, R. *Angew. Chem. Int. Ed.***1963**, *2*(10), 565.doi: 10.1002/anie.196305651.

40. Jin, T.;Yan, M.;Yamamoto, Y. *Chem. Cat. Chem.***2012**, *4*(9), 1217.doi: 10.1002/cctc.201200193.

41. Heravi, M. M.;Hashemi, E.;Beheshtiha, S. Y.;Ahmadi, S.;Hosseinnejad, T. *J. Mol. Cat. A.***2014**, *394*, 74.doi:10.1016/j.molcata.2014.07.001.

42. Hosseinnejad, T.; *Mol. Cryst. Liq. Cryst.* **2014**, *605*, 89. doi: 10.1080/15421406.2014.904995.

43. Mirsafaei, R.; Heravi, M. M.; Ahmadi, S.; Hosseinnejad, T. *Chem. Pap.* **2016**, *70*(4), 418. doi:10.1515/chempap-2015-0228.

44. Mirsafaei, R.; Heravi, M. M.; Hosseinnejad, T.;Ahmadi, S. *Appl. Organomet. Chem*. **2016**, *30*(10), 823. doi: 10.1002/aoc.3509.

45. Hosseinnejad, T.; Dinyari, M. *Comput. Theor. Chem.* **2015**, *1071*, 53. doi: 10.1016/j.comptc.2015.08.014.

46. Hosseinnejad, T.; Dehghanpour, S.; Hosseinjani, A. *Comput. Theor. Chem.* **2013**, *1004*, 31.doi: 10.1016/j.comptc.2012.10.011.

47. Hosseinnejad, T.; Kazemi, T. *Mol. Cryst. Liq. Cryst.* **2016**, *637*(1), 53. doi: 10.1080/15421406.2016.1206807.

48. Lee, C.;Yang, W. R.;Parr, G. *Phys. Rev. B.* **1988**, *37*(2), 785.doi:10.1103/PhysRevB.37.785.

49. Bader, R. F. W. Atoms in Molecules: a Quantum Theory, Oxford University Press, Oxford, UK, 1990.

50. Truhlar, D.G.;Zhao, Y. *Theor. Chem. Account.***2008**, *120*(1), 215.doi:10.1007/s00214-007-0310-x.

51. Schmidt, M.W.; Baldridge, K.K.; Boatz, J.A.; Elbert, S.T.; Gordon, M.S.; Jensen, J.H.;Koseki, S.;Matsunaga, N.;Nguyen, K.A.; Su, S.;Windus, T.L.;Dupuis, M.;MontgomeryJr, J.A. *J. Comput. Chem.***1993**,*14*(11), 1347.doi: 10.1002/jcc.540141112.

52. Barone, V.;Cossi, M. *J. Phys. Chem. A.***1998**, *102*(11), 1995.doi: 10.1021/jp9716997.

53. Bader, R. F. W. AIM2000 Program, ver 2.0, Hamilton, McMaster University, 2000.

54. Yuan, B.;He, R.;Shen, W.; Huang, C.;Li, M. *J. Org. Chem.***2015**, *80*(13), 6553.doi: 10.1021/acs.joc.5b00523.

55. Heravi, M. M.; Behbahani, F. K.;Oskooie, H. A.; HekmatShoar, R. *Tetrahedron Lett.***2005**, *46*(16), 2775. doi: 10.1016/j.tetlet.2005.02.147.

56. Heravi, M. M.; Bakhtiari, K.; Javadi, N. M.; Bamoharram, F. F.; Saeedi, M.; Oskooie, H. A. *J. Mol. Catal. A: Chem.***2007**, *264*(1-2), 50.doi: 10.1016/j.molcata.2006.09.004.

57. Zare, A.;Abi, F.;Moosavi-Zare, A. R.;Beyzavi, M. H.;Zolfigol, M. A. *J. Mol. Liq.***2013**, *178*, 113.doi: 10.1016/j.molliq.2012.10.045.

58. Nasr-Esfahani, M.;Hoseini, S. J.;Montazerozohori, M.;Mehrabi, R.;Nasrabadi, H. *J. Mol. Catal. A: Chem.***2014**, *382*, 99.doi: 10.1016/j.molcata.2013.11.010.

59. Kidwai, M.;Bhatnagar, D. *Chem. Pap.***2010**, *64*(6), 825. doi: 10.2478/s11696-010-0070-2.

60. Debache, A.;Boulcina, R.;Belfaitah, A.;Rhouati, S.;Carboni, B. *Synlett***2008**, *2008*(4), 0509.doi: 10.1055/s-2008-1032093.

Tables:

Table 1.M06/6-311+G** calculated values of bond order and bond length for some selected key bonds in SMI ligand, N-CuI/SMI and O-CuI/SMI complexes. Note that the calculated bond length values have been presented in the parenthesis. Numbering of atoms is in accordance with Figure 1.

	SMI ligand	N-CuI/SMI complex	O-CuI/SMI complex
N1-C2	1.339(1.332)	1.317(1.345)	1.388(1.320)
N1-C3	1.391(1.333)	1.288(1.344)	1.430(1.318)
N2-C4	0.847(1.420)	0.912(1.412)	1.067(1.411)
N2-C5	0.808(1.407)	0.870(1.395)	0.951(1.389)
N2-C6	0.710(1.405)	0.706(1.412)	0.622(1.413)
C5-O1	2.440(1.205)	2.509(1.185)	2.352(1.212)
C6-O2	2.433(1.205)	2.518(1.186)	2.409(1.220)
Cu-N1	------	0.512(1.907)	------
Cu-O1	------	------	0.171(2.099)
Cu-I	------	1.337(2.490)	1.396(2.458)

Table 2. The bond orders of Cu-N and Cu-O chemical bonds in DMF and ethanol solution phases, calculated at M06/6-311+G** level of theory *via* PCM approach

	Cu-N N-CuI/SMI complex	Cu-O O-CuI/SMI complex
Ethanol	0.562	0.229
DMF	0.594	0.243

Table 3. Mathematical properties of BCPs associated to some selected bonds in SMI ligand, N-CuI/SMI and O-CuI/SMI complexes. The properties have been obtained *via* QTAIM analysis on M06/6-311+G**calculated wave functions of electron density. Note that numbering of atoms is in accordance with Figure 2.

	ρ_b	$\nabla^2\rho_b$	G_b	V_b	H_b	$\|V_b\|/G_b$
SMI ligand						
N_1-C_2	0.3469	-0.8428	0.3394	-0.8895	-0.5501	2.6208
N_1-C_3	0.3473	-0.8462	0.3393	-0.8902	-0.5509	2.6236
C_5-O_1	0.4225	-0.0427	0.7238	-1.4583	-0.7345	2.0147
C_6-O_2	0.4218	-0.0360	0.7234	-1.4560	-0.7326	2.0127
N-CuI/SMI complex						
N_1-C_2	0.3449	-0.6968	0.3741	-0.9226	-0.5485	2.4661
N_1-C_3	0.3454	-0.6978	0.3749	-0.9243	-0.5494	2.4654
Cu-N_1	0.0954	0.4106	0.1451	-0.1877	-0.0426	1.2935
Cu-I	0.0586	0.1232	0.0740	-0.0900	-0.0159	1.2154
O-CuI/SMI complex						
C_5-O_1	0.4236	-0.0700	0.7499	-1.4823	-0.7324	1.9766
C_6-O_2	0.4421	-0.1520	0.8185	-1.5990	-0.7805	1.9535
Cu-O_1	0.0532	0.2899	0.0864	-0.1004	-0.0139	1.1614
Cu-I	0.0636	0.1125	0.0534	-0.0787	-0.0253	1.4738

Table 4. Optimization of reaction conditions for the synthesis of **1a**

Entry	Solvent	Temperature (°C)	Time (min)	Yield (%)^a
1	-	60	55	78
2	**-**	**80**	**30**	**92**
3	Water	Reflux	45	83
4	Ethanol	Reflux	35	80
5	Acetonitrile	Reflux	80	68
6	H_2O/EtOH (1:1)	Reflux	50	85

^{a}Yields of isolated pure products

Table 5. The effect of different amount of CuI/SMI nanocatalyst on the synthesis of substituted 1,4-dihydropyridine **1a**

Entry	Catalyst amount (g)	Time (min)	Yield (%)^a
1	0.020	55	76
2	0.030	45	87
3	**0.040**	**30**	**92**
4	0.050	35	90

^{a}Yields of isolated pure products

Table 6. Synthesis of substituted 1,4-DHP derivatives **1a-r** in the presence of CuI/SMI nanocatalyst

Product	R	Compound 3		Time (min)	Yield (%)[a]	Mp (°C)	Mp (Lit.)
1a	H	Dimedone	Ethyl acetoacetate	30	92	206-208	206-208[57]
1b	4-Cl	Dimedone	Ethyl acetoacetate	30	90	244-246	244-246[57]
1c	4-MeO	Dimedone	Ethyl acetoacetate	35	89	255-256	255-257[57]
1d	H	Dimedone	Methyl acetoacetate	45	85	261-262	260-262[57]
1e	4-Cl	Dimedone	Methyl acetoacetate	35	90	220-221	220-221[58]
1f	4-Me	Dimedone	Methyl acetoacetate	40	88	274-276	275-276[58]
1g	H	Dimedone	Dimedone	30	89	278-280	279-280[59]
1h	3-F	Dimedone	Dimedone	25	93	298-300	New
1i	4-Cl	Dimedone	Dimedone	25	91	298-299	297-299[59]
1j	2-MeO	Dimedone	Dimedone	30	90	293-295	293-295[59]
1k	H	Methyl acetoacetate	Methyl acetoacetate	40	84	115-117	115-117[58]
1l	4-Cl	Methyl acetoacetate	Methyl acetoacetate	35	80	197-198	196-198[58]
1m	4-NO_2	Methyl acetoacetate	Methyl acetoacetate	40	81	166-168	167-169[58]
1n	4-MeO	Methyl acetoacetate	Methyl acetoacetate	30	87	186-188	186-188[58]
1o	H	Ethyl acetoacetate	Ethyl acetoacetate	30	90	157-158	156-158[60]

1p	4-Cl	Ethyl acetoacetate	Ethyl acetoacetate	35	88	145-147	144-146[60]
1q	4-MeO	Ethyl acetoacetate	Ethyl acetoacetate	30	90	157-158	157-159[60]
1r	3-Me	Ethyl acetoacetate	Ethyl acetoacetate	30	91	123-124	122-124[60]

[a] Yields of isolated pure products

Figure captions:

Figure1. Atomic numbering and optimized structures obtained at M06/6-31G* level of theory for SMI ligand, N-CuI/SMI and O-CuI/SMI complexes

Figure2. Complete molecular graphs (MGs) of SMI ligand, N-CuI/SMI and O-CuI/SMI complexes obtained by QTAIM analysis of M06/6-311+G** electron density functions. Bond Critical Points: red circles; Ring Critical Points: yellow circles; Bond Paths: pink lines.

Figure3. The recyclability of the CuI/SMI nanocatalyst in the synthesis of **1a**

Graphical Abstract

Computational investigations on structural and electronic properties of CuI nanoparticles immobilized on modified poly(styrene-co-maleic anhydride), leading to unexpected but an efficient catalyzed synthesis 1,4-dihydropyridine via Hantzsch reaction

Majid M. Heravi, Tayebeh Hosseinnejad*, Niousha Nazari*

Department of Chemistry, Alzahra University, Vanak, Tehran, Iran